

•Original article•

## Stigmasterol protects human brain microvessel endothelial cells against ischemia-reperfusion injury through suppressing EPHA2 phosphorylation

LI Suping<sup>1</sup>, XU Fei<sup>1</sup>, YU Liang<sup>1</sup>, YU Qian<sup>2</sup>, YU Nengwei<sup>1</sup>, FU Jing<sup>2\*</sup><sup>1</sup>Department of Neurology, Sichuan Academy of Medical Sciences & Sichuan Provincial People's Hospital, Chengdu 610072, China;<sup>2</sup>Department of Rehabilitation, Sichuan Academy of Medical Sciences & Sichuan Provincial People's Hospital, Chengdu 610072, China

Available online 20 Feb., 2023

**[ABSTRACT]** Stigmasterol is a plant sterol with anti-apoptotic, anti-oxidative and anti-inflammatory effect through multiple mechanisms. In this study, we further assessed whether it exerts protective effect on human brain microvessel endothelial cells (HBMECs) against ischemia-reperfusion injury and explored the underlying mechanisms. HBMECs were used to establish an *in vitro* oxygen and glucose deprivation/reperfusion (OGD/R) model, while a middle cerebral artery occlusion (MCAO) model of rats were constructed. The interaction between stigmasterol and EPHA2 was detected by surface plasmon resonance (SPR) and cellular thermal shift assay (CETSA). The results showed that 10  $\mu\text{mol}\cdot\text{L}^{-1}$  stigmasterol significantly protected cell viability, alleviated the loss of tight junction proteins and attenuated the blood-brain barrier (BBB) damage induced by OGD/R in the *in vitro* model. Subsequent molecular docking showed that stigmasterol might interact with EPHA2 at multiple sites, including T692, a critical gatekeep residue of this receptor. Exogenous ephrin-A1 (an EPHA2 ligand) exacerbated OGD/R-induced EPHA2 phosphorylation at S897, facilitated ZO-1/claudin-5 loss, and promoted BBB leakage *in vitro*, which were significantly attenuated after stigmasterol treatment. The rat MCAO model confirmed these protective effects *in vivo*. In summary, these findings suggest that stigmasterol protects HBMECs against ischemia-reperfusion injury by maintaining cell viability, reducing the loss of tight junction proteins, and attenuating the BBB damage. These protective effects are at least mediated by its interaction with EPHA2 and inhibitory effect on EPHA2 phosphorylation.

**[KEY WORDS]** Stigmasterol; Oxygen and glucose deprivation/reperfusion; EPHA2; Blood-brain barrier

**[CLC Number]** R965    **[Document code]** A    **[Article ID]** 2095-6975(2023)02-0127-09

### Introduction

Endothelial cells (ECs) are a critical component of the blood-brain barrier (BBB) [1]. The BBB integrity is essential for the homeostasis and normal function of the central nervous system (CNS). Acute ischemic stroke is associated with endothelial dysfunction and subsequent BBB leakage, leading to edema around the ischemic area [2]. BBB leakage and edema may be reversible when the triggering factors are appropriately handled at the early stage [2]. However, if the triggering factors are severe and consistently exist, cell-to-cell junctions may be disrupted. Apoptotic and pyroptotic en-

dothelial cells may detach from the vessel wall, resulting in vascular structural alterations [2]. These pathological changes then cause vascular fragility and subsequent development of hemorrhages [2].

Stigmasterol is a plant sterol that can not be biosynthesized by the human body. It is obtained from dietary sources of phytosterols and absorbed through the intestines [3]. Recent studies have reported that stigmasterol exhibits brain protective effects after stroke through complex mechanisms [4-6]. Stigmasterol exerted neuroprotective effect against ROS-induced damage in rats after stroke through reducing oxidative stress and suppressing autophagy [4]. It also bound to and activated sirtuin 1, which helped ameliorate oxidative stress-induced neuronal cell death [6]. Furthermore, it induced mitophagy in primary rat hippocampal neurons after ischemia-reperfusion through binding to the ligand binding domain of liver X receptor  $\beta$  (LXR $\beta$ ) and acted as an agonist [5]. Therefore, stigmasterol may be a promising natural compound with therapeutic potential in neurological diseases.

**[Received on]** 17-Sep.-2022

**[Research funding]** This work was supported by the Key Research Project of the Science & Technology Department of Sichuan Province, China (Nos. 2021YFS0131 and 2020YFS0414).

**[\*Corresponding author]** E-mail: 2091145921@qq.com

These authors have no conflict of interest to declare.

With respect to its anti-oxidant and anti-inflammatory effect, we hypothesize that stigmaterol may exert protective effect on human brain microvessel endothelial cells (HBMECs), thereby protecting the BBB integrity after ischemia-reperfusion. The regulatory effect of a natural compound primarily relies on its docking proteins and the downstream signaling pathways [7]. However, the docking proteins of stigmaterol are still not fully understood in neurological diseases. The Ephrin-Eph signaling cascade has been considered as a novel pathway involved in ischemic stroke [8]. Among the Ephrin receptors, EPHA2 was activated after ischemic stroke and promoted vascular inflammation and permeability in a murine stroke model [9].

In this study, we investigated the protective effect of stigmaterol on HBMECs against oxygen and glucose deprivation/reperfusion (OGD/R) induced injury and the docking proteins involved. Meanwhile, a middle cerebral artery occlusion (MCAO) model of rats was constructed to validate the *in vivo* protective effect.

## Materials and Methods

### Cell culture

Human brain microvessel endothelial cells (HBMECs) were purchased from Procell (CP-H124, Wuhan, China) and cultured in the recommended medium (CM-H124, Procell) in a 37 °C incubator with 5% CO<sub>2</sub>. The purity of the cells was validated by immunofluorescence staining of CD31 (Supplementary Fig. 1). Stigmaterol (purity: 99.07%) and ALW-II-41-27 (a potent inhibitor of EPHA2) were purchased from Selleck (Houston, TX, USA). Recombinant human ephrin-A1 Fc chimera protein was purchased from R&D System (6417-A1-050).

### *In vitro* OGD/R model

HBMECs were cultured in 24-well transwell plates/inserts or 6-well plates until 70%–80% confluence. For the group treated with stigmaterol (2 or 10 μmol·L<sup>-1</sup> as indicated in figure legends), stigmaterol was added to the culture medium 12 h before OGD/R. Then, the cells were washed and cultured in glucose-free culture medium in a hypoxic chamber (1% O<sub>2</sub>, 5% CO<sub>2</sub> and 94% N<sub>2</sub>) for 2 or 4 h. Then, the cells were incubated under the normal condition for an additional 12 h, with the same concentrations of stigmaterol during this period.

### Trans-Endothelial Electrical Resistance (TEER) assay

TEER assay was conducted using a Millipore Millicell ERS system equipped with chopstick electrodes (Millipore, Billerica, MA, USA), according to previous methods [10]. Briefly, 2 × 10<sup>5</sup> HBMECs in 0.5 mL culture medium were grown on the top chamber surface of 24-well Transwell inserts (12 mm Transwell with 0.4 μm Pore Polyester Membrane Insert, Corning Incorporated, Corning, NY, USA) to form a monolayer. The same culture medium (1.5 mL) was filled into the lower chamber. TEER value was measured daily to record the time of peak resistance (reported as Ω/cm<sup>2</sup>). Then, the chamber carrying HBMEC monolayer was

subjected to OGD/R, with or without the presence of indicated stigmaterol (2 or 10 μmol·L<sup>-1</sup>).

### Determination of paracellular permeability through quantifying the diffusion of FITC-dextran

The diffusion of FITC-dextran (70 kDa; Sigma-Aldrich, St. Louis, MO, USA) across the HBMEC monolayer was determined to assess paracellular permeability, according to previous description [11]. In brief, the Transwell inserts with HBMEC monolayer were first pretreated with stigmaterol (2 or 10 μmol·L<sup>-1</sup>) for 12 h and then subjected to OGD/R. Afterward, they were transferred into new wells filled with pre-warmed HBSS buffer for washing. FITC-dextran (1 mg·mL<sup>-1</sup>) was added to the upper chamber and then incubated at 37 °C for 60 min in the darkness. Then, the solution in the lower chambers was transferred into a new black 96-well plate to measure fluorescence intensity on a fluorescence microplate reader (excitation at 492 nm and emission at 518 nm, BioTek Synergy Neo2, Agilent Technologies, Santa Clara, CA, USA). Relative fluorescence intensity was represented as fold-change.

### Immunofluorescence staining

Immunofluorescence staining was performed according to previous methods [12]. HBMECs were grown on coverslips in a 24-well plate and subjected to OGD (2 h)/R (12 h), with or without the presence of 10 μmol·L<sup>-1</sup> stigmaterol. The cells were then fixed with 4% paraformaldehyde, permeabilized in 0.1% Triton X-100, and blocked with 10% goat serum. The coverslips were incubated with rabbit CoraLite594-Conjugated ZO-1 polyclonal antibody (1 : 200, CL594-21773, Proteintech, Wuhan, China) and mouse Alexa Fluor 488-Conjugated claudin-5 monoclonal antibody (1 : 2000, 352588, Thermo Fisher Scientific, Wortham, TX, USA) at 4 °C overnight. For brain rat tissues, they were first paraffin-embedded and then sectioned. Immunofluorescence staining was performed according to previous description [13]. The tissue sections were incubated with mouse ZO-1 monoclonal antibody (1 : 100, 14-9776-82, Thermo Fisher Scientific) and rabbit anti-p-EPHA2 (1 : 200, #6347, Cell Signaling Technology, Danvers, MA, USA) at 4 °C overnight. The secondary CoraLite594-conjugated Goat Anti-Mouse IgG (H + L) and CoraLite488-conjugated Goat Anti-Rabbit IgG (H + L) were used. After three times washing with PBS, the coverslips were mounted using ProLong Gold Antifade Mountant with DAPI (Thermo Fisher Scientific, Wortham, TX, USA). The fluorescence was examined under a confocal microscope (FV1000, Olympus, Tokyo, Japan).

### Western blot

Western blot was conducted as previously described [12]. Briefly, 30 μg protein per sample was loaded and separated using SDS-polyacrylamide gel electrophoresis. Then, the samples were transferred onto nitrocellulose membrane. The following primary antibodies were used: anti-EPHA2 (1 : 1000, #6997, Cell Signaling Technology), anti-p-EPHA2 (1 : 1000, #6347, Cell Signaling Technology), anti-ZO-1 (1 : 1000, #5406, Cell Signaling Technology), anti-claudin-5 (1 : 1000, A10207, ABclonal, Wuhan, China), anti-ROCK1 (1 : 2000, 21850-1-AP, Proteintech) and anti-ROCK2 (1 : 1000,

20248-1-AP, Proteintech). The protein bands were developed using chemiluminescence reagents (BeyoECL Star, Beyotime, Shanghai, China). Protein expression was quantified by densitometry and normalized to  $\beta$ -actin using ImageJ software (version 1.37, NIH, Bethesda, MD, USA).

#### Cellular thermal shift assay (CETSA)

CETSA was conducted as previously described [14]. In brief, 10  $\mu\text{mol}\cdot\text{L}^{-1}$  stigmaterol or vehicle control (DMSO) was incubated with the cellular lysate supernatant of HBMECs at room temperature for 1 h. Then, five aliquot samples (50  $\mu\text{L}$ ) were heated at 45, 55, 60, 65, or 70  $^{\circ}\text{C}$  respectively (5 min) and cooled at room temperature (5 min). The samples were centrifuged for Western blot to detect the presence of EPHA2.  $\beta$ -Actin served as the negative control. All uncropped blot images are shown in Supplementary Fig. 2.

#### Identification of the potential docking proteins of stigmaterol by bioinformatic analysis

The potential docking proteins of stigmaterol were predicted using SwissTargetPrediction (<http://swisstargetprediction.ch/>) [15] and SEA (Similarity ensemble approach) (<http://sea.bkslab.org/>) [16]. For docking prediction, the structure of stigmaterol was transferred to SMILES chemical format (CC[C@H](C=C[C@@H](C)[C@H]1CC[C@@H]2[C@@]1(CC[C@H]3[C@H]2CC=C4[C@@]3(CC[C@@H](C4)O)C)C(C)C) for docking prediction. Then, the specific atomic interaction between stigmaterol and EPHA2 was conducted using CB-Dock (<http://clab.labshare.cn/cb-dock/php/index.php>) [17]. Moreover, 5I9W in RCSB PDB (PDB DOI: 10.2210/pdb5I9W/pdb) was used for docking, which is a crystal structure of EPHA2 with ANP (Phosphoaminophosphonic Acid-Adenylate Ester). The genes encoding the predicted targeting proteins were used for Gene Ontology (GO) and Kyoto Encyclopedia of Genes and Genomes (KEGG) analysis using R package “clusterProfiler” (v 3.14.3).

#### Surface plasmon resonance (SPR) analysis

SPR analysis was performed using a Biacore T200 (GE Healthcare, Pittsburgh, PA, USA), human recombinant EPHA2 protein (P29317, R&D System, Minneapolis, MN, USA) and a CM5 chip, according to a standard amine coupling procedure as previously described [14].

#### Flow cytometry

Apoptotic cells were measured by Annexin V/PI staining. HBMECs were subjected to OGD (2 h)/R (12 h), with or without the presence of stigmaterol (10  $\mu\text{mol}\cdot\text{L}^{-1}$ ). For the groups treated with exogenous ephrin-A1, HBMECs were exposed to ephrin-A1 (2.5  $\mu\text{g}\cdot\text{mL}^{-1}$ ) for 30 min after OGD. Then, the cells were harvested, washed and incubated with 5  $\mu\text{L}$  of Annexin V-FITC and 10  $\mu\text{L}$  of PI (20  $\mu\text{g}\cdot\text{mL}^{-1}$ ) in 100  $\mu\text{L}$   $1\times$  binding buffer at room temperature for 15 min in the darkness. Then, 400  $\mu\text{L}$  PBS was added to each sample. The cells were analyzed by a FACSCalibur flow cytometer (Becton, Dickinson and Company, San Diego, CA, USA), with 488-nm excitation and a 525-nm filter for FITC and a 620-nm filter for PI detection.

#### MCAO in rats

All animal studies and experimental procedures fol-

lowed the NIH Guide for the Care and Use of Laboratory Animals (8<sup>th</sup> edition) and were approved by the Ethics Committee of Sichuan Provincial People's Hospital, China (Approval No. 2021226). Male Sprague-Dawley rats (220–250 g) were purchased from Chengdu Dashuo Biotechnology Co., Ltd. (Chengdu, China). The dose of stigmaterol (3  $\text{mg}\cdot\text{kg}^{-1}$ ) and ephrin-A1 (10  $\text{mg}\cdot\text{kg}^{-1}$ ) were determined based on the recommendations in previous publications [18, 19]. A MCAO model of rats was constructed as previously described [12]. The rats were randomly divided into five groups: (1) Sham group ( $n = 6$ ), with the sham operation; (2) MCAO/R alone ( $n = 6$ ); (3) MCAO/R + intravenous injection (i.v.) of ephrin-A1 (10  $\text{mg}\cdot\text{kg}^{-1}$ , 30 min before occlusion,  $n = 6$ ); (4) MCAO/R + intraperitoneal injection (i.p.) of stigmaterol (3  $\text{mg}\cdot\text{kg}^{-1}$ , 30 min before occlusion,  $n = 6$ ); (5) MCAO/R + simultaneous i.v. of ephrin-A1 (10  $\text{mg}\cdot\text{kg}^{-1}$ ) and i.p. of stigmaterol (3  $\text{mg}\cdot\text{kg}^{-1}$ , 30 min before occlusion,  $n = 6$ ). After 90 min of occlusion, the monofilament was gently removed to restore blood supply for 72 h. Then, the rats were euthanized to collect the brain tissues. Five brains per group were used for 2,3,5-triphenyltetrazolium chloride (TTC) staining to determine the infarct volume. The tissues in the penumbra area after TTC staining were removed and subjected to Western blot, as TTC staining has limited influence on Western blot results [20]. One rat brain from each group was fixed, embedded in paraffin, and sectioned for immunofluorescence staining of p-EPHA2 and ZO-1.

#### Statistical analysis

All data were analyzed by GraphPad Prism 8.01 software (GraphPad Software, San Diego, CA, USA). Multiple group comparisons were conducted using one-way ANOVA test, followed by the Tukey post hoc test. Welch's unpaired  $t$ -test was used for two-group comparisons. Data are expressed as the mean  $\pm$  standard derivation (SD).  $P < 0.05$  was considered significant.

## Results

#### Stigmaterol protects HBMEC against OGD/R-induced injury by mitigating the degradation of tight junction proteins

The chemical structure of stigmaterol is presented in Fig. 1A. According to previous publications, the optimal neuroprotective concentration of stigmaterol was between 2.50–150  $\mu\text{mol}\cdot\text{L}^{-1}$  [5]. To identify appropriate concentrations of stigmaterol for this study, the effect of four different concentrations of stigmaterol on the viability of HBMECs was evaluated by Cell Counting Kit-8 (CCK-8) assay (Fig. 1B). The results showed that no significant alterations on HBMEC viability were seen after treatment with 2 or 10  $\mu\text{mol}\cdot\text{L}^{-1}$  stigmaterol for 24 h. In contrast, treatment with 50 and 100  $\mu\text{mol}\cdot\text{L}^{-1}$  stigmaterol for 24 h substantially decreased the viability (Fig. 1B). Then, HBMECs were subjected to OGD/R with or without the presence of stigmaterol. OGD/R significantly impaired cell viability and increased LDH release (Figs. 1C–1D). However, 10  $\mu\text{mol}\cdot\text{L}^{-1}$  stigmaterol remarkably rescued cell viability and decreased LDH release after OGD/R (Figs. 1C–1D).

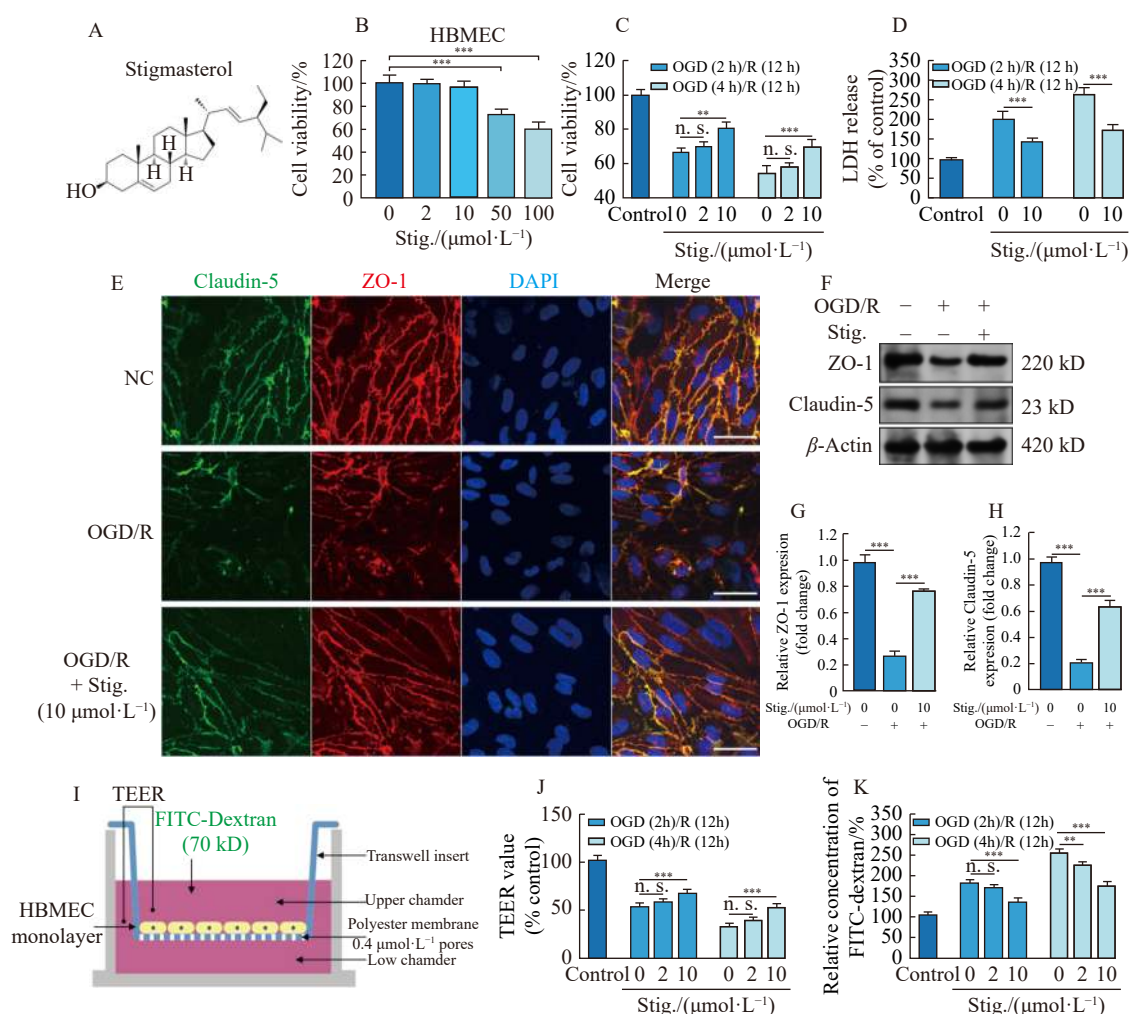


**Fig. 1** Stigmasterol protects HBMECs against OGD/R induced injury by mitigating the degradation of tight junction proteins. **A**, The chemical structure of stigmasterol. **B**, Effect of different concentrations of stigmasterol (2, 10, 50, and 100  $\mu\text{mol}\cdot\text{L}^{-1}$ ) treatment (24 h) on the viability of HBMECs. **C–D**, CCK-8 assay (**C**) and LDH release assay (**D**) were performed to evaluate the protective effects of stigmasterol against OGD/R-induced reduction of cell viability in different OGD/R groups. **E–H**, Representative immunofluorescent images (**E**) and Western blot assay (**F–H**) showing the expression of claudin-5 (green) and ZO-1 (red) in HBMECs after OGD (2 h)/R (12 h), with or without the presence of stigmasterol (10  $\mu\text{mol}\cdot\text{L}^{-1}$ ). **I**, Illustration of the *in vitro* BBB model. HBMECs were seeded on the top side of the Transwell insert to form a monolayer. Then, TEER values and paracellular diffusion of FITC-dextran (70 kDa) were measured. **J–K**, TEER values (**J**) and relative concentration of FITC-dextran (**K**) were calculated to evaluate the protective effect of stigmasterol against OGD/R-induced disruption of barrier function in different OGD/R groups. Scale bar = 20  $\mu\text{m}$ . Stig.: Stigmasterol. Data are expressed as the mean  $\pm$  SD ( $n = 3$ ). \*\* $P < 0.01$ , \*\*\* $P < 0.001$  vs controls (n.s.: not significant)

Next, we assessed the influence of stigmasterol on the expression of claudin-5 and ZO-1, two important tight junction proteins in maintaining the BBB integrity [21]. Immunofluorescence labeling and subsequent Western blot assay revealed that stigmasterol attenuated OGD/R-induced downregulation of ZO-1 and claudin-5 in HBMECs (Figs. 1E–1H). Then, HBMECs were grown in Transwell inserts and allowed to form a monolayer, until the peak TEER was reached (Fig. 1I). Then, the monolayer was subjected to OGD/R with or without the presence of stigmasterol. Then, TEER values were determined again and the results showed that stigmasterol partly restored TEER drop due to OGD/R (Figs. 1I–1J). FITC-dextran diffusion assay also confirmed that stigmasterol

significantly alleviated OGD/R-induced transmembrane penetration of FITC-dextran (Figs. 1I and 1K).

#### Identification of the potential docking proteins of stigmasterol by bioinformatic analysis

To explore the potential docking proteins of stigmasterol, bioinformatic prediction was conducted using SwissTargetPrediction (<http://swisstargetprediction.ch/>) and SEA (Similarity ensemble approach) (Fig. 2A). A total of 72 nonredundant candidates were identified (Supplementary Table 1). Then, the genes encoding these proteins were used for GO/KEGG analysis (Fig. 2B). Detailed information and the genes involved in the GO/KEGG terms were provided in Supplementary Table 2. Transmembrane ephrin receptor activity and

ephrin receptor activity were the major molecular function (MF) terms (Fig. 2B, red frames). Through molecular docking, we found that stigmasterol might interact with EPHA2 at multiple sites. Notably, stigmasterol might directly interact with Thr692 (T692) (Fig. 2C, red arrow), which is the gatekeeper residue of EPHA2<sup>[22]</sup>. In addition, this binding position of stigmasterol is quite similar to the known binding of ANP to EPHA2<sup>[22]</sup> (Fig. 2D). Surface plasmon resonance data showed that stigmasterol interacted with recombinant human EPHA2 protein in a concentration-dependent manner ( $K_D = 8.6 \pm 0.7 \mu\text{mol} \cdot \text{L}^{-1}$ , Fig. 2E). According to CETSA results, stigmasterol increased the thermal stability of EPHA2 protein, compared with DMSO control (Fig. 2F).

#### Stigmasterol protects the BBB integrity *in vitro* by reducing OGD/R-induced EPHA2 phosphorylation

Ephrin-A1 is a physiological ligand of EPHA2 receptor<sup>[8]</sup>. Western blot results showed that OGD/R induced significant

upregulation of EPHA2 and p-EPHA2. Stigmasterol did not affect EPHA2 expression but significantly decreased OGD/R-induced EPHA2 phosphorylation (Figs. 3A–3B). Furthermore, exogenous ephrin-A1 exacerbated OGD/R-induced EPHA2 phosphorylation at Ser897 and ZO-1/claudin-5 downregulation. These changes were reversed by stigmasterol treatment (Figs. 3A–3E). Similar to ALW-II-41-27, stigmasterol inhibited the phosphorylation of EPHA2 and suppressed the expression of Rho-associated coiled coil-containing protein kinases 1 and 2 (ROCK1 and ROCK2) (Fig. 3F), two known downstream effectors of EPHA2 in endothelial cells<sup>[23]</sup>. Through TEER and FITC-dextran diffusion assays, we observed that exogenous ephrin-A1 exacerbated OGD/R-induced downregulation of TEER values and upregulation of FITC-dextran transmembrane permeability (Figs. 3G–3H). However, these alterations were significantly reversed by stigmasterol or ALW-II-41-27 treatment (Figs. 3G–3H).

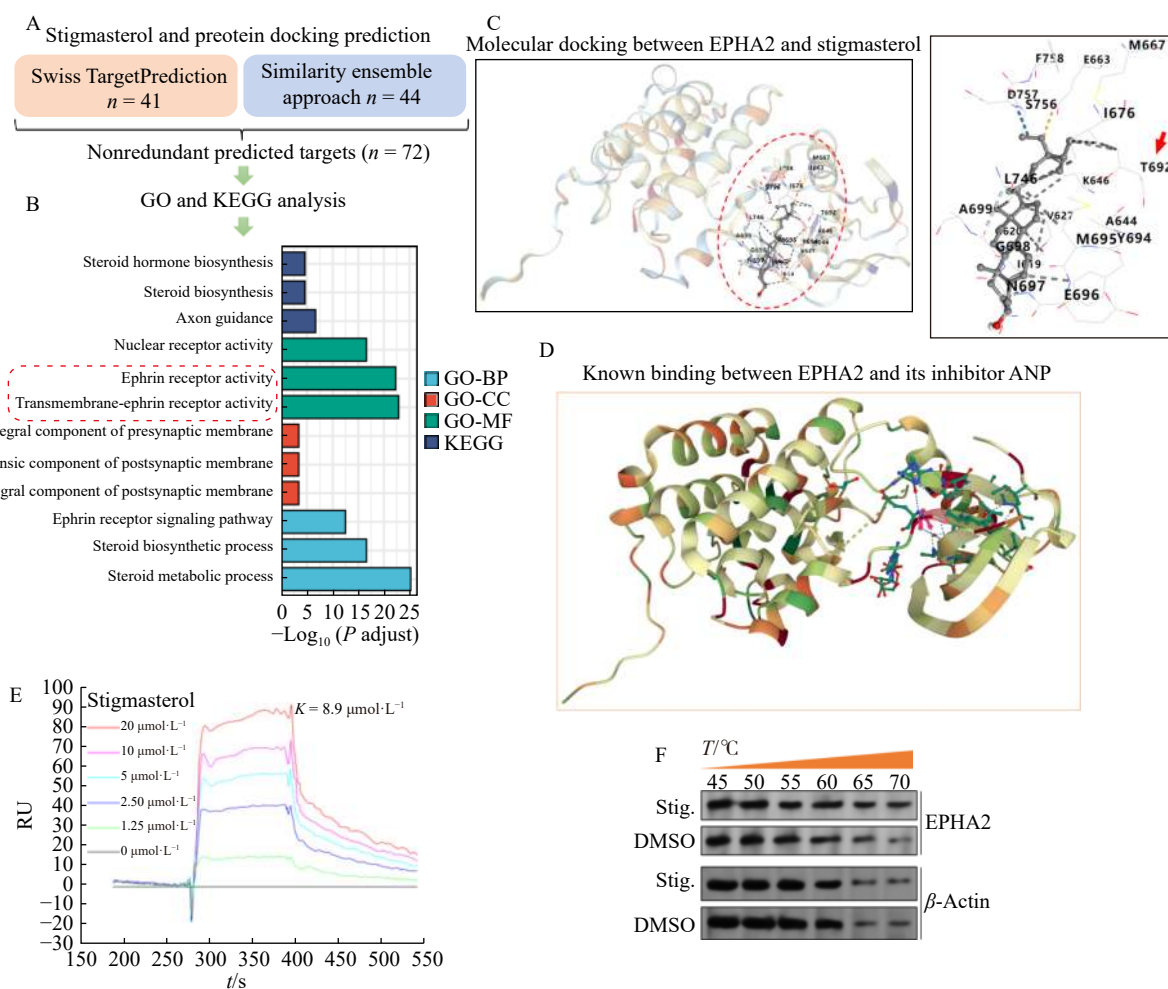


**Fig. 2** Stigmasterol binds to EPHA2 with a high affinity. **A**, Bioinformatic prediction using SwissTargetPrediction (<http://swisstargetprediction.ch/>) and SEA (Similarity ensemble approach) to identify the potential stigmasterol docking proteins. **B**, A bar chart showing the enrichment of the 72 nonredundant candidates in GO/KEGG terms. **C**, Molecular docking analysis showing a typical stigmasterol potential binding site on EPHA2, which covers the gatekeeper T692 site. **D**, The known binding between ANP and EPHA2 (which can be accessed from: <https://www.rcsb.org/structure/5I9W>). **E**, SPR analysis of the binding of stigmasterol to human recombinant EPHA2 protein. **F**, Representative images of CETSA of EPHA2 with 10  $\mu\text{mol} \cdot \text{L}^{-1}$  stigmasterol or DMSO control.  $\beta$ -Actin was used as the loading control

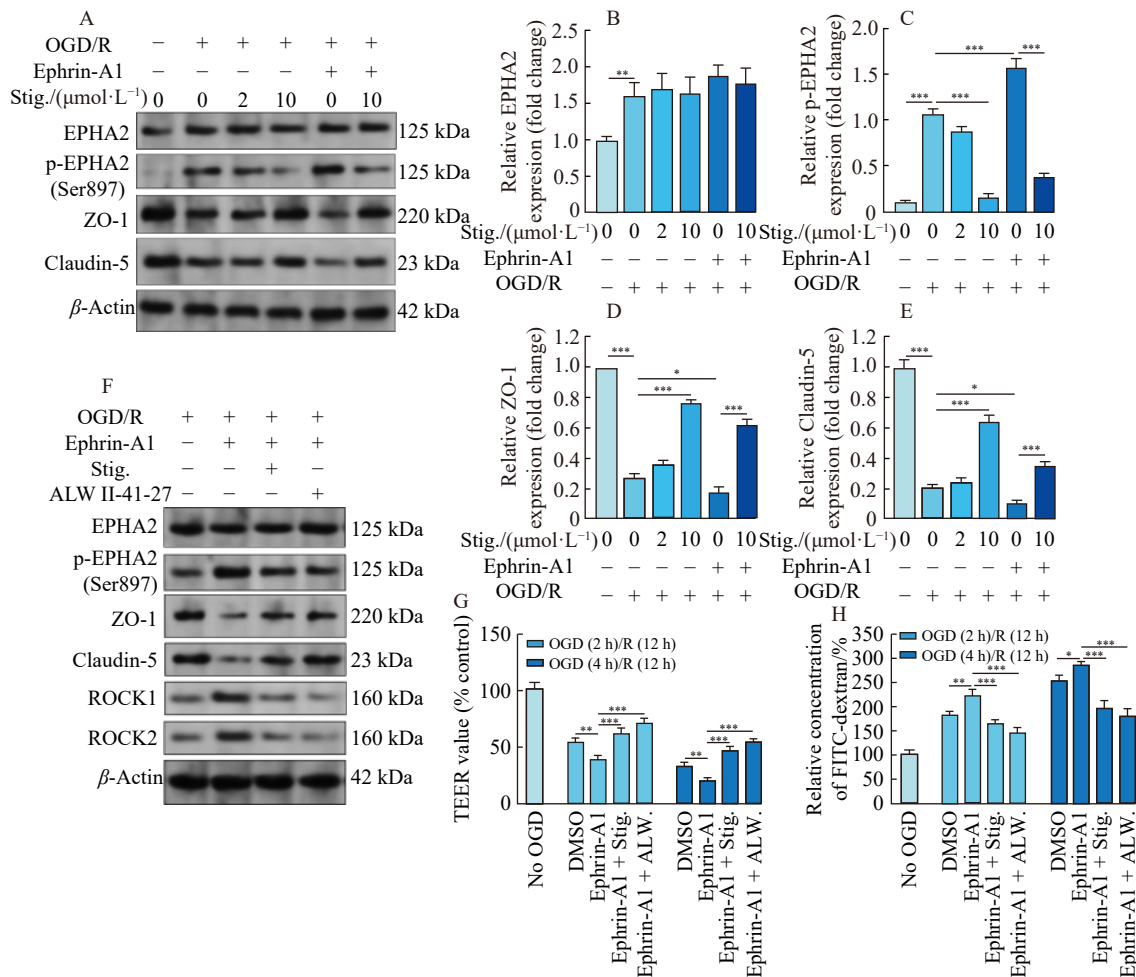


**Fig. 3** Stigmasterol protects the BBB integrity *in vitro* by reducing OGD/R-induced EPHA2 phosphorylation. A–E, Representative images (A) and bar plots (B–E) showing the relative expression of EPHA2, p-EPHA2, ZO-1 and claudin-5 in HBMECs after OGD (2 h)/R (12 h), with or without the presence of stigmasterol (2 or 10  $\mu\text{mol}\cdot\text{L}^{-1}$ ). For the groups with exogenous ephrin-A1 exposure, HBMEC monolayers were treated with ephrin-A1 (2.5  $\mu\text{g}\cdot\text{mL}^{-1}$ ) for 30 min after OGD. (F) Representative images showing the expression of EPHA2, p-EPHA2, ZO-1, claudin-5, ROCK1 and ROCK2 in HBMECs after OGD (2 h)/R (12 h), with indicated selective combinations of stigmasterol (10  $\mu\text{mol}\cdot\text{L}^{-1}$ ), ephrin-A1 (2.5  $\mu\text{g}\cdot\text{mL}^{-1}$ ) or ALW-II-41-27 (2  $\mu\text{mol}\cdot\text{L}^{-1}$ ). For the groups with ALW-II-41-27 exposure, ALW-II-41-27 (2  $\mu\text{mol}\cdot\text{L}^{-1}$ ) was administered together with ephrin-A1 (2.5  $\mu\text{g}\cdot\text{mL}^{-1}$ ) for 30 min after OGD. (G–H) Relative TEER values (G) and relative concentration of FITC-dextran (H) were calculated to evaluate the protective effect of stigmasterol against OGD/R-induced disruption of barrier function in different OGD/R groups, with indicated selective combinations of stigmasterol (10  $\mu\text{mol}\cdot\text{L}^{-1}$ ), ephrin-A1 (2.5  $\mu\text{g}\cdot\text{mL}^{-1}$ ) or ALW-II-41-27 (2  $\mu\text{mol}\cdot\text{L}^{-1}$ ). Stig.: Stigmasterol; ALW.: ALW-II-41-27. Data are expressed as the mean  $\pm$  SD ( $n = 3$ ). \* $P < 0.05$ , \*\* $P < 0.01$ , \*\*\* $P < 0.001$  vs controls (n.s.: not significant)

#### Stigmasterol protects HBMECs against OGD/R-induced apoptosis

Next, we assessed whether stigmasterol protected HBMECs against OGD/R-induced apoptosis. The results showed that OGD/R stimulated increased production of pro-inflammatory mediators, including IL-1 $\beta$ , MCP-1, TNF- $\alpha$ , and IL-6 (Figs. 4A–4D). These changes were enhanced by ephrin-A1 treatment but were attenuated by stigmasterol treatment (Figs. 4A–4D). Stigmasterol treatment also reduced the ratio of Annexin V<sup>+</sup>/PI<sup>−</sup> (early apoptosis) and Annexin V<sup>+</sup>/PI<sup>+</sup> (late apoptosis) in HBMECs induced by OGD/R and exacerbated by ephrin-A1 (Fig. 4E–4F).

#### Stigmasterol protects the BBB integrity *in vivo*

To explore the protective effect of stigmasterol on the

BBB integrity *in vivo*, a MCAO/R model of rats was established. The results showed that exogenous ephrin-A1 increased infarcted volume, while stigmasterol treatment reduced infarcted volume and partly reversed the detrimental effects of ephrin-A1 (Figs. 5A–5B). Through immunofluorescence staining, we examined the expression of p-EPHA2 and ZO-1 in the penumbra area. The results indicated that ephrin-A1 treatment exacerbated the morphological alterations (loss of integrity and continuity) of the microvessels induced by MCAO/R (reflected by ZO-1 staining) (Fig. 5C). When ephrin-A1 was given, the levels of p-EPHA2 significantly increased (Figs. 5C–5D and 5G). Its co-localization with ZO-1 was observed (Fig. 5C, white arrows). Stigmasterol treatment reduced EPHA2 phosphorylation and protected the

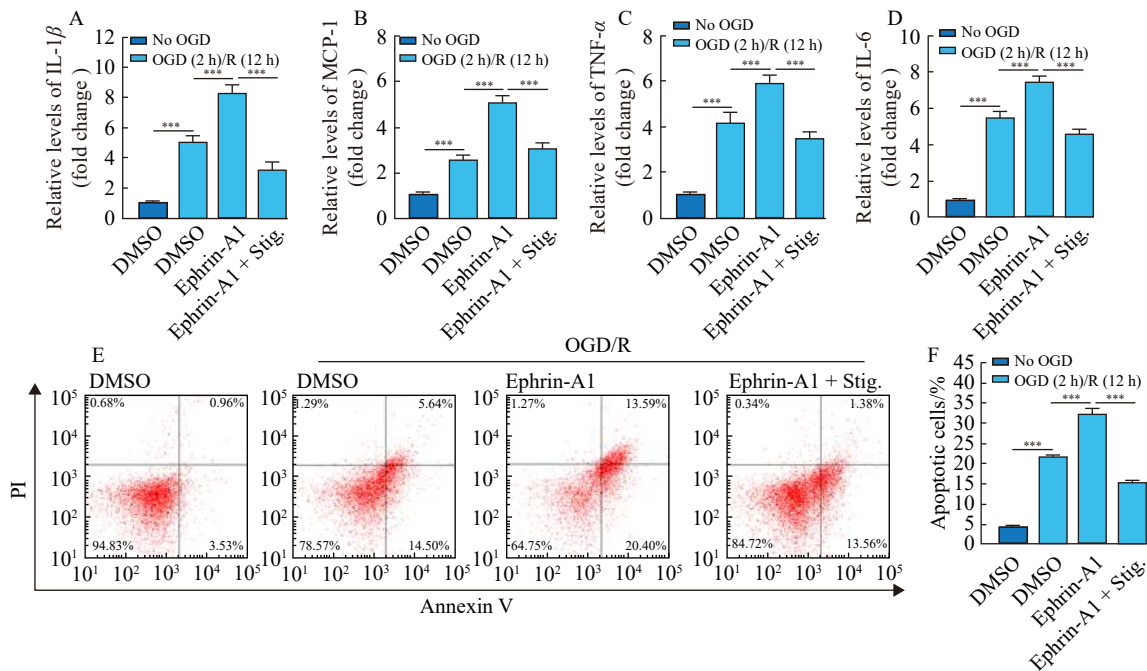


**Fig. 4** Stigmasterol protects HBMECs against OGD/R-induced apoptosis. (A–D) Levels of pro-inflammatory mediators in HBMECs induced by OGD/R (2 h OGD followed by 12 h reoxygenation), with or without the presence of stigmasterol (10  $\mu\text{mol}\cdot\text{L}^{-1}$ ). (E–F) Representative images (E) and summarized data showing cell apoptosis determined by flow cytometry in HBMECs with indicated treatments. Data are expressed as the mean  $\pm$  SD ( $n = 3$ ). \*\*\*  $P < 0.001$  vs controls

morphological integrity of the brain microvessels (Fig. 5C). Western blot results also demonstrated that stigmasterol significantly suppressed EPHA2 phosphorylation and alleviated the loss of ZO-1/claudin-5 (Figs. 5D–5H).

## Discussion

Stigmasterol has been considered as a neuroprotective agent after ischemic stroke [4-6, 24], but its potential protective effect on HBMECs have not been completely explored. The current study was designed to investigate the effect of stigmasterol on HBMECs after OGD/R. The results showed that 10  $\mu\text{mol}\cdot\text{L}^{-1}$  stigmasterol significantly protected cell viability, alleviated the loss of tight junction proteins and attenuated *in vitro* BBB damage after OGD/R.

Stigmasterol may exert anti-apoptotic antioxidative and anti-inflammatory effect through multiple mechanisms. In the neurons, it might interact with Sirt1 and attenuate oxidative stress-induced injury through activating SIRT1-deacetylation reaction on its target protein and increasing FoxO3a expression [6]. It interacted with Relin receptor ApoER2 and activated the downstream signaling molecules, such as c-Jun *N*-terminal kinase, doublecortin and dynein heavy chain in migratory neurons [25]. It also bound to LXR $\beta$  and acted as an agonist [5]. It exhibited significant anxiolytic and anticonvulsant effect by binding to and positively modulating multiple gamma-aminobutyric acid A receptors [18]. Recent network pharmacological studies have suggested that stigmasterol may have multiple docking proteins, such as EGFR, SRC, ESR, MTOR, ERBB2, MCL1, MMP9, KDR, JAK2, CASP3, and MAPK8 [26-28]. These findings imply that the docking protein network of stigmasterol is complex.

To explore the docking proteins of stigmasterol involved in OGD/R-induced endothelial cell injury, we performed docking analysis and identified 72 potential candidates. Subsequent GO/KEGG analysis confirmed that transmembrane ephrin receptor activity and ephrin receptor activity were the major molecular MF terms, which are novel pathways involved in ischemic stroke [8]. Molecular docking analysis showed that stigmasterol might interact with EPHA2 at multiple sites, including T692, a critical gatekeep residue of this receptor. Previous studies demonstrated the regulatory effect of EPHA2 on vascular injury and leakage. In a rat model of lung injury induced by hypoxia, EPHA2 was upregulated and associated with vascular leak [29]. Another study showed that EPHA2 $^{-/-}$  mice have decreased vascular permeability in bleomycin-induced lung injury [30]. EPHA2 expression was elevated after ischemia/reperfusion in brain tissues in a murine stroke model, which promoted vascular inflammation and permeability [9]. Knocking down EPHA2 in HBMECs facilitated tight junction formation and prevented ephrin-A1-induced disruption of tight junctions [31]. Furthermore, one study generated ephrin-A1 mutants (EMs) and found one mutant (EM2), which reduced EPHA2 phosphorylation and exhibited potent neuroprotective effect in a mouse focal ischemia/reperfusion (I/R) model [19]. EM2 reduced brain infarct volume, neuronal apoptosis, and cerebral edema and improved neurological scores. In addition, this mutant also decreased BBB leakage and inflammatory infiltration, with better preservation of tight junction proteins [19]. Therefore, developing EPHA2 antagonists is considered a potential strategy to explore new neuroprotective agents. EPHA2 is proposed as the major candidate docking protein of stig-

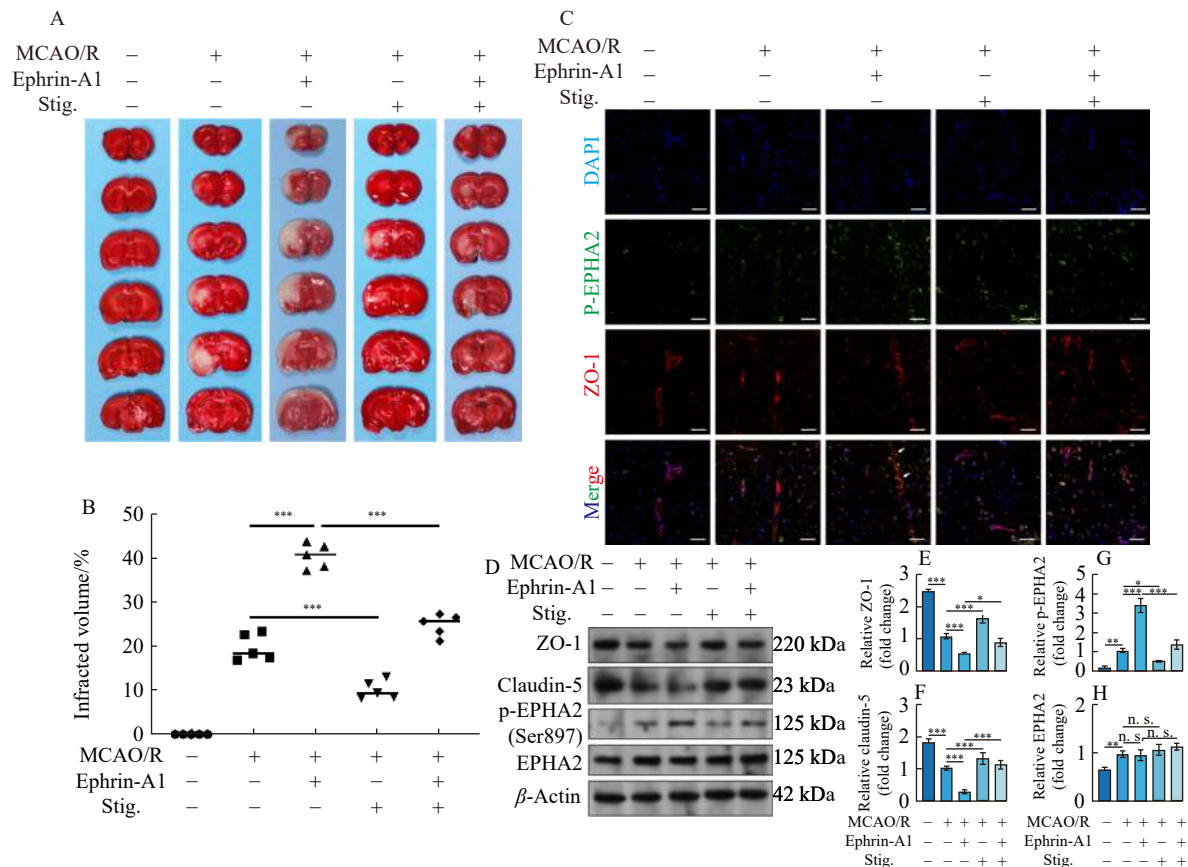


**Fig. 5** Stigmasterol protects the BBB integrity *in vivo*. (A–B) Representative images of TTC staining (A) and quantitation (B) of the ipsilateral stroke infarct volumes of rat brains with indicated treatments ( $n = 5$ , the other brain was paraffin-embedded for immunofluorescence staining). The white (unstained) areas indicate infarction, while the red (stained) areas indicate normal tissue. (C) Immunofluorescence staining of p-EPHA2 (green) and ZO-1 (red) in the penumbra area (Scale bar = 100  $\mu\text{m}$ ). (D–H) Representative images (D) and bar plots (E–H) of the relative expression of ZO-1 (E), claudin-5 (F), p-EPHA2 (G) and EPHA2 (H) in the ipsilateral ischemic hemisphere (mainly the penumbra area) from each group in panel A. Data are expressed as the mean  $\pm$  SD ( $n = 3$ ). \*  $P < 0.05$ , \*\*  $P < 0.01$ , \*\*\*  $P < 0.001$  vs controls (n.s.: not significant)

masterol for further studies.

Previous studies showed that ligand-dependent phosphorylation of EPHA2 at Ser897 was involved in hyperhomocysteinemia-induced endothelial cell injury [32]. Therefore, we examined whether stigmasterol regulated EPHA2 phosphorylation at this site. The results demonstrated that exogenous ephrin-A1 exacerbated OGD/R-induced EPHA2 phosphorylation at Ser897, facilitated ZO-1/claudin-5 loss, and BBB leakage *in vitro*, which were significantly attenuated after stigmasterol treatment. Inhibiting ROCK1 and ROCK2 might abrogate all of the detrimental effects of ephrin-A1 on the BBB model *in vitro* [23], suggesting that ROCK1/2 proteins are the critical downstream effectors of EPHA2. Furthermore, our data indicated that stigmasterol suppressed the expression of ROCK1/2, similar to the effect of ALW-II-41-27. Then, the rat MCAO model confirmed the protective effects of stigmasterol on the integrity of rat brain microvessels *in vivo*. Therefore, stigmasterol may serve as a potential agent to protect HBMECs against ischemia-reperfusion injury through suppressing EPHA2 phosphorylation.

As mentioned above, stigmasterol may regulate complex signaling pathways *via* different docking proteins. It attenu-

ated the phosphorylation of FAK, PCL, SRC, and VEGFR2 in some tumors [33, 34]. In the acute phase of stroke, the intrinsic elevation of VEGFA and subsequent VEGFR2 phosphorylation led to BBB leakage [35, 36]. Since stigmasterol has known inhibitory effect on the VEGF signaling pathway, this mechanism may also contribute to BBB protection. Therefore, future studies are required to expand our understanding of the regulatory network of stigmasterol in neurological disorders.

## Conclusion

This study demonstrates that stigmasterol protects HBMECs against ischemia-reperfusion injury through maintaining cell viability, reducing the loss of tight junction proteins, and attenuating the BBB damage. This protective effect is at least mediated by its interaction with EPHA2 and inhibitory effect on EPHA2 phosphorylation.

## Supporting Information

Supporting information of this paper can be requested by sending E-mails to the corresponding authors.

## References

- [1] Andjelkovic AV, Xiang J, Stamatovic SM, et al. Endothelial targets in stroke: translating animal models to human [J]. *Arterioscler Thromb Vasc Biol*, 2019, **39**(11): 2240-2247.
- [2] Maeda KJ, McClung DM, Showmaker KC, et al. Endothelial cell disruption drives increased blood-brain barrier permeability and cerebral edema in the Dahl SS/jr rat model of superimposed preeclampsia [J]. *Am J Physiol Heart Circ Physiol*, 2021, **320**(2): H535-H548.
- [3] Heinemann T, Axtmann G, von-Bergmann K. Comparison of intestinal absorption of cholesterol with different plant sterols in man [J]. *Eur J Clin Invest*, 1993, **23**(12): 827-831.
- [4] Sun J, Li X, Liu J, et al. Stigmasterol exerts neuro-protective effect against ischemic/reperfusion injury through reduction of oxidative stress and inactivation of autophagy [J]. *Neuropsychiatr Dis Treat*, 2019, **15**: 2991-3001.
- [5] Haque MN, Hannan MA, Dash R, et al. The potential LXRbeta agonist stigmasterol protects against hypoxia/reoxygenation injury by modulating mitophagy in primary hippocampal neurons [J]. *Phytomedicine*, 2021, **81**: 153415.
- [6] Pratiwi R, Nantasenamat C, Ruankham W, et al. Mechanisms and neuroprotective activities of stigmasterol against oxidative stress-induced neuronal cell death via sirtuin family [J]. *Front Nutr*, 2021, **8**: 648995.
- [7] Temml V, Schuster D. Chapter 18, *Molecular Docking for Natural Product Investigations: Pitfalls and Ways to Overcome Them. Molecular Docking for Computer-Aided Drug Design* [M]. Academic Press, 2021: 391-405.
- [8] Elgebaly MM. Ephrin-eph signaling as a novel neuroprotection path in ischemic stroke [J]. *J Mol Neurosci*, 2020, **70**(12): 2001-2006.
- [9] Thundyil J, Manzanero S, Pavlovski D, et al. Evidence that the EphA2 receptor exacerbates ischemic brain injury [J]. *PLoS One*, 2013, **8**(1): e53528.
- [10] Srinivasan B, Kolli AR, Esch MB, et al. TEER measurement techniques for *in vitro* barrier model systems [J]. *J Lab Autom*, 2015, **20**(2): 107-126.
- [11] Hu S, Wu Y, Zhao B, et al. *Panax notoginseng* saponins protect cerebral microvascular endothelial cells against oxygen-glucose deprivation/reperfusion-induced barrier dysfunction via activation of PI3K/Akt/Nrf2 antioxidant signaling pathway [J]. *Molecules*, 2018, **23**(11): 2781.
- [12] Li S, Fu J, Wang Y, et al. LncRNA MIAT enhances cerebral ischaemia/reperfusion injury in rat model via interacting with EGLN2 and reduces its ubiquitin-mediated degradation [J]. *J Cell Mol Med*, 2021, **25**(21): 10140-10151.
- [13] Zaqout S, Becker LL, Kaindl AM. Immunofluorescence staining of paraffin sections step by step [J]. *Front Neuroanat*, 2020, **14**: 582218.
- [14] Li S, Yu N, Xu F, et al. Ginsenoside Rd protects cerebral endothelial cells from oxygen-glucose deprivation/reoxygenation induced pyroptosis via inhibiting SLC5A1 mediated sodium influx [J]. *J Ginseng Res*, 2022, **46**(5): 700-709.
- [15] Daina A, Michielin O, Zoete V. SwissTargetPrediction: updated data and new features for efficient prediction of protein targets of small molecules [J]. *Nucleic Acids Res*, 2019, **47**(W1): W357-W364.
- [16] Keiser MJ, Roth BL, Armbruster BN, et al. Relating protein pharmacology by ligand chemistry [J]. *Nat Biotechnol*, 2007, **25**(2): 197-206.
- [17] Liu Y, Grimm M, Dai WT, et al. CB-Dock: a web server for cavity detection-guided protein-ligand blind docking [J]. *Acta Pharmacol Sin*, 2020, **41**(1): 138-144.
- [18] Karim N, Khan I, Abdelhalim A, et al. Stigmasterol can be new steroidal drug for neurological disorders: evidence of the GABAergic mechanism via receptor modulation [J]. *Phytomedicine*, 2021, **90**: 153646.
- [19] Zhu Y, Gao Y, Zheng D, et al. Design and evaluation of EphrinA1 mutants with cerebral protective effect [J]. *Sci Rep*, 2017, **7**(1): 1881.
- [20] Sanchez-Bezanilla S, Nilsson M, Walker FR, et al. Can we use 2,3,5-triphenyltetrazolium chloride-stained brain slices for other purposes? The application of western blotting [J]. *Front Mol Neurosci*, 2019, **12**: 181.
- [21] Lv J, Hu W, Yang Z, et al. Focusing on claudin-5: a promising candidate in the regulation of BBB to treat ischemic stroke [J]. *Prog Neurobiol*, 2018, **161**: 79-96.
- [22] Heinzlmeir S, Kudlinzki D, Sreeramulu S, et al. Chemical proteomics and structural biology define EPHA2 inhibition by clinical kinase drugs [J]. *ACS Chem Biol*, 2016, **11**(12): 3400-3411.
- [23] Zhao Y, Li W, Song J, et al. High expression of EphA2 led to secondary injury by destruction of BBB integrity through the ROCK pathway after diffuse axonal injury [J]. *Neurosci Lett*, 2020, **736**: 135234.
- [24] Liang Q, Yang J, He J, et al. Stigmasterol alleviates cerebral ischemia/reperfusion injury by attenuating inflammation and improving antioxidant defenses in rats [J]. *Biosci Rep*, 2020, **40**(4): BSR20192133.
- [25] Haque MN, Moon IS. Stigmasterol promotes neuronal migration via reelin signaling in neurosphere migration assays [J]. *Nutr Neurosci*, 2020, **23**(9): 679-687.
- [26] Wang Y, Zhang Y, Wang Y, et al. Using network pharmacology and molecular docking to explore the mechanism of Shan-Ci-Gu (*Crematista appendiculata*) against non-small cell lung cancer [J]. *Front Chem*, 2021, **9**: 682862.
- [27] Wang Y, Yuan Y, Wang W, et al. Mechanisms underlying the therapeutic effects of Qingfei Yin in treating acute lung injury based on GEO datasets, network pharmacology and molecular docking [J]. *Comput Biol Med*, 2022, **145**: 105454.
- [28] Zhou M, Li J, Luo D, et al. Network pharmacology and molecular docking-based investigation: prunus mume against colorectal cancer via silencing RelA expression [J]. *Front Pharmacol*, 2021, **12**: 761980.
- [29] Cercone MA, Schroeder W, Schomberg S, et al. EphA2 receptor mediates increased vascular permeability in lung injury due to viral infection and hypoxia [J]. *Am J Physiol Lung Cell Mol Physiol*, 2009, **297**(5): L856-863.
- [30] Carpenter TC, Schroeder W, Stenmark KR, et al. Eph-A2 promotes permeability and inflammatory responses to bleomycin-induced lung injury [J]. *Am J Respir Cell Mol Biol*, 2012, **46**(1): 40-47.
- [31] Zhou N, Zhao WD, Liu DX, et al. Inactivation of EphA2 promotes tight junction formation and impairs angiogenesis in brain endothelial cells [J]. *Microvasc Res*, 2011, **82**(2): 113-121.
- [32] Tian D, Qin Q, Li M, et al. Homocysteine impairs endothelial cell barrier function and angiogenic potential via the progranulin/EphA2 pathway [J]. *Front Pharmacol*, 2021, **11**: 614760.
- [33] Kangsamaksin T, Chaithongyot S, Wootthichairangsan C, et al. Lupeol and stigmasterol suppress tumor angiogenesis and inhibit cholangiocarcinoma growth in mice via downregulation of tumor necrosis factor- $\alpha$  [J]. *PLoS One*, 2017, **12**(12): e0189628.
- [34] Michelini FM, Lombardi MG, Bueno CA, et al. Synthetic stigmasterol derivatives inhibit capillary tube formation, herpetic corneal neovascularization and tumor induced angiogenesis: antiangiogenic stigmasterol derivatives [J]. *Steroids*, 2016, **115**: 160-168.
- [35] Geiseler SJ, Morland C. The janus face of VEGF in stroke [J]. *Int J Mol Sci*, 2018, **19**(5): 1362.
- [36] Wu L, Ye Z, Pan Y, et al. Vascular endothelial growth factor aggravates cerebral ischemia and reperfusion-induced blood-brain-barrier disruption through regulating LOC102640519/HOXC13/ZO-1 signaling [J]. *Exp Cell Res*, 2018, **369**(2): 275-283.

**Cite this article as:** LI Suping, XU Fei, YU Liang, YU Qian, YU Nengwei, FU Jing. Stigmasterol protects human brain microvessel endothelial cells against ischemia-reperfusion injury through suppressing EPHA2 phosphorylation [J]. *Chin J Nat Med*, 2023, **21**(2): 127-135.